

Accuracy of Inverse Solution Computation of Dominant Frequencies and Phases during Atrial Fibrillation

J Pedrón-Torrecilla¹, AM Climent², A Liberos¹, M Rodrigo¹, E Pérez-David², J Millet¹,
F Fernández-Avilés², O Berenfeld³, F Atienza², MS Guillem¹

¹ ITACA, Universitat Politècnica de Valencia, Valencia, Spain

² Cardiology Department, Hospital General Universitario Gregorio Marañón, Madrid, Spain

³ Center for Arrhythmia Research, University of Michigan, Ann Arbor, USA

Abstract

Ablation of sources identified by dominant frequency (DF) or phase analyses in patients with atrial fibrillation (AF) is proposed as a therapy to terminate the arrhythmia. The aim of this study was to evaluate non-invasive identification of AF sources by solving the inverse problem. Realistic mathematical models of atria and torso anatomy with different DF patterns of AF were used. For these models inverse-computed electrograms EGMs were compared to intracardiac EGMs in terms of their voltage, phase and frequency spectrum errors. In models without added noise, atrial spectrums were estimated with lower relative errors than phases (3.8±3.8 vs 41±17 % respectively, p<0.01) and after noise addition differences between relative errors of spectrums and phases were more pronounced (5.5±4.1 vs 48±14 %, respectively p<0.01). Non-invasive location of the highest DF during AF showed a better accuracy than in the phase and voltage domain, being a promising clinical tool for identification of sources prior to ablation.

1. Introduction

Atrial fibrillation (AF) has a great clinical impact in morbidity and mortality in developed countries [1]. Treatment with antiarrhythmic drugs is not always effective and has many secondary effects. These limitations have led to the development of new therapeutic strategies, such as radiofrequency ablation with current success rates in arrhythmia control of 50 to 80 % [1]. Among different radiofrequency ablation strategies, ablation of high frequency sources has proved to be particularly effective in case that these high frequency sources can be identified [2]. These high frequency sources are usually located near the pulmonary veins (PVs) [3] but they can be located anywhere in the atria [4]. A non-invasive identification of these high frequency sources by solving the inverse problem of the

electrocardiography prior to the clinical procedure could be used as guidance to plan the ablation procedure.

Previous studies on inverse problem resolution during AF have shown paradoxically simple activation patterns [5,6], which do not correspond with the complex propagation patterns recorded epicardially [7] and which have not been validated by using simultaneous intracardiac data. Recently we have described the mechanisms by which the estimation of detailed voltage and phase propagation patterns during AF from noninvasive recordings may be limited [8]. For these reasons, the acceptance of the inverse-problem resolution as a guidance for AF ablation is still controversial.

In this article, we aim to compare AF source estimation by non-invasive DF maps reconstruction by solving the inverse problem of the electrocardiography and the more commonly used phase and voltage maps reconstruction, determining the noise sensitivity and their percentage error.

2. Methods

2.1. Inverse problem resolution

In order to obtain the potentials on the heart surface from the potentials recorded non-invasively from the torso surface of the patient, we solved the inverse problem of the electrocardiography based on the Boundary Element Method (BEM).

According to the BEM formulation [9,10], potentials on the surface of the torso can be computed from potentials on the heart surface by using (1)-(3):

$$mx = b \quad (1)$$

$$m = \begin{pmatrix} D_{AA(nxn)} & G_{AA(nxn)} \\ D_{TA(mxn)} & G_{TA(mxn)} \end{pmatrix}, \quad x = \begin{pmatrix} \Phi_A \\ \Gamma_A \end{pmatrix}, \quad b = \begin{pmatrix} -D_{AT(nxm)} \Phi_T \\ -D_{AT(mxm)} \Phi_T \end{pmatrix} \quad (2)$$

$$\Phi_T = M\Phi_A = (D_{TT} - G_{TA}G_{AA}^{-1}D_{AT})^{-1} \cdot (G_{TA}G_{AA}^{-1}D_{AA} - D_{TA})\Phi_A \quad (3)$$

where Φ_A is the potential on the surface of the atria, Φ_T is the potential on the surface of the torso, Γ_A is the potential gradient in the atria, D_{TA} and D_{AT} are the potential transfer matrices from the torso to the atria and from the atria to the torso respectively, and G_{TA} and G_{AT} are the potential gradient transfer matrices from the torso to the atria and from the atria to the torso respectively.

The inverse problem could be solved by computing the inverse of matrix M (M^{-1}). However, M is ill-conditioned and, in order to overcome the ill-conditioned nature of M , the system needs to be regularized. We accomplished this regularization by using zero-order Tikhonov's method, which consists of a minimization problem, according to Equation 4:

$$\min \left\{ \|M \Phi_A - \Phi_T\|^2 + \lambda \|B \Phi_A\|^2 \right\} \quad (4)$$

where λ is a regularization parameter that we automatically obtained by the L-curve method [11] and B is a spatial regularization matrix, which is the identity matrix in zero-order formulation. Therefore, the inverse problem can be solved by using Equation 5:

$$\Phi_H(t) = (M^T M + \lambda B^T B)^{-1} M^T \Phi_T \quad (5)$$

2.2. Inverse problem validation

Several surface potential distributions were calculated by solving the forward problem of the electrocardiography, using realistic atria, which consisted of 577264 nodes and its size was 12.5x9 cm [12]. The action potential of each node was simulated by using a mathematical model which includes ionic currents, pumps and exchangers, and processes regulating intracellular concentration changes of Na^+ , K^+ and Ca^{2+} [13]. The whole tissue is described as a monodomain model. After discretization of the spatial derivatives for an isotropic medium, the evolution of the transmembrane voltage of each cell (i.e. V_i for the i -th cell) V_i , was controlled by the following first-order, time-dependent ordinary differential equation:

$$\frac{dV_i}{dt} = \frac{I_{total,i}}{C_m} - D \sum_j \frac{V_i - V_j}{d_{i,j}} \quad (6)$$

where D describes the diffusion of voltage through the medium, $I_{total,i}$ summarizes the contribution of all transmembrane currents [13], C_m is the transmembrane capacitance, and $d_{i,j}$ is the distance between neighbor cells i and j .

Atrial fibrillation in the realistic model was induced in-silico by a S1-S2 stimulation protocol. Two S1 stimulations with a period of 100 ms and a pulse duration of 5 ms were applied at either the left superior pulmonary

veins or the sinus node, depending on the desired pattern. A rectangular shape stimulus S2 was applied 70 ms after the last S1 stimulus with a duration of 2 ms in the same S1 pacing site, inducing the AF. The model incorporated an extra potassium current, the acetylcholine (ACh) potassium current (IKacg). This current produces a shortening in the action potential which favors the occurrence of arrhythmic behavior and the presence of different activation frequencies [2].

Mathematical computations were performed by using an adaptive time-step solver on a Graphical Processing Unit [14]. Transmembrane potentials were computed for a simulation time of 5 seconds after stabilization of the model and were resampled to 1 kHz.

Simulated electrograms (EGMs) (i.e. 5988 signals for the realistic atria) were calculated by using transmembrane potentials generated by the cellular mathematical model [12]:

$$EGM = \sum_{\vec{r}} \left(\frac{\vec{r}}{r^3} \right) \cdot \vec{\nabla} V_m \quad (7)$$

where \vec{r} is the distance vector between the measuring point and a point in the tissue domain (r is the euclidean distance -1 mm-), $\vec{\nabla}$ denotes the gradient operator, and V_m is the transmembrane potential.

Body surface potential signals were computed on the outer surface from EGMs by solving the forward problem with the Boundary Element Method [9,10]. Specifically, ECGs on a realistic torso model with 771 nodes and 1538 faces were estimated [15]. Simulated ECGs were used to estimate the inverse computed epicardial electrograms (icEGM) by solving the inverse problem of the electrocardiography. In order to evaluate the performance of the inverse problem under a realistic noisy situation, icEGM were calculated before and after the addition of 10 dBs white noise.

Simulated EGMs and inverse-computed EGMs were compared in terms in the voltage, phase and spectral domains. Instantaneous phase, which ranges from 0 to 2π and represents the relative delay of each signal in one period, was computed in each node by using the Hilbert transform [8]. Frequency analysis was performed by computing the power spectral density of all signals by using Welch's periodogram with a Hamming window of 2 seconds and 50 % overlap, with 8192 FFT points per window (0.25 Hz of frequency resolution). The largest peak in each spectrum was defined as the dominant frequency of the node. Accuracy of reconstructed EGMs was quantified by measuring the percentage of reconstructed error between normalized voltage, phase and spectrum (from 3 to 20 Hz) of original intracardiac recordings and icEGM. The t-test was used to evaluate the statistical significance between the errors for the three domains (i.e. voltage, phase and frequency).

3. Result

Voltage, phase and DF maps computed for the realistic atrial and torso models are depicted in Figure 1 and 2. Resulting AF patterns were: (1) AF generated by a rotor located in the left atrium (LA), with a DF of 12.25 Hz in the LA and 8 Hz in the RA, as depicted in Figure 1, (2) AF generated by a rotor located in the RA, with a DF of 12.25 Hz in the RA and 8 Hz in the LA, as depicted in Figure 2.

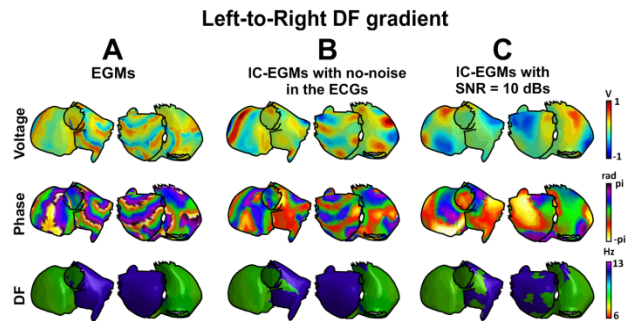


Figure 1. Inverse-computed voltage, phase and dominant frequency (DF) maps for simulated AF with a left-to-right DF gradient. *Panel A:* Voltage, phase and DF maps for generated epicardial electrograms (EGM). *Panel B:* Voltage, phase and DF maps for inverse computed electrograms (icEGM) without added noise. *Panel C:* Voltage, phase and DF maps for icEGM with added noise on surface potentials at 10 dBs SNR.

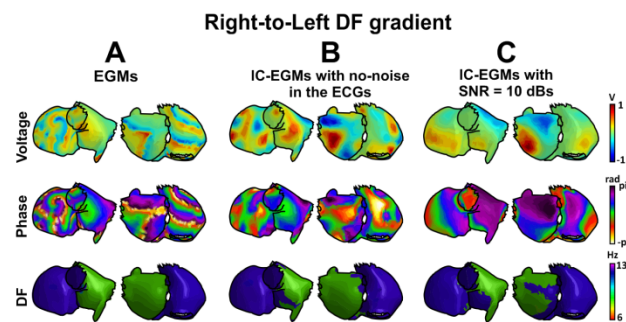


Figure 2. Inverse-computed voltage, phase and dominant frequency (DF) maps for simulated AF with a right-to-left DF gradient. *Panel A:* Voltage, phase and DF maps for generated epicardial electrograms (EGM). *Panel B:* Voltage, phase and DF maps for inverse computed electrograms (icEGM) without added noise. *Panel C:* Voltage, phase and DF maps for icEGM with added noise on surface potentials at 10 dBs SNR.

As it can be observed without added noise, inverse-computed voltages and phases represent a smoothed version of modelled epicardial potentials and while some activation wavefronts can be estimated some other wavefronts are missed, as depicted in Figure 1 and 2.

Epicardial potentials reconstructed after addition of noise at 10 dB SNR present an increased smoothing of both voltage distribution and phase to an extent at which activation wavefronts do not match after forward and inverse problem resolution. Dominant frequency estimation was again performed accurately for most of the atrial surface, although some errors are found at some atrial sites, as depicted in Figure 1 and 2.

As it can be concluded from the data in Figure 3, in which the performance of the estimation of EGMs in the two presented models is summarized. When no noise is added to the ECGs, frequency reconstruction is more robustly estimated by the inverse problem than voltage or phase (3.8 ± 3.4 % error for spectrums vs. 31 ± 15 % error for voltage and 41 ± 17 % error for phase, $p < 0.01$). When 10 dBs noise is added, frequency reconstruction is also more robustly estimated (5.5 ± 4.1 % error for spectrums vs. 38 ± 15 % error for voltage and 48 ± 14 % error for phase, $p < 0.01$).

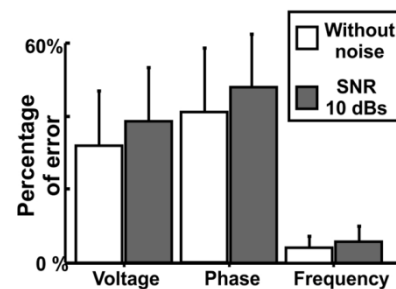


Figure 3. Comparison between simulated and inverse-computed EGMs. Percentage of error between inverse computed electrograms (icEGM) and original electrograms (EGM) with and without the addition of SNR white noise of 10 dBs to the surface electrocardiograms.

4. Discussion and conclusions

The main finding of the present study is that a noninvasive estimation of activation frequencies in the atria by solving the inverse problem of the electrocardiography is feasible and can be used to compute frequency maps, identifying AF sources. We have shown that inverse quantification of atrial patterns during AF in the frequency domain is more accurate than estimation of voltage distributions or their instantaneous phase.

During the last years, several groups have developed and tested the methodology to noninvasively reconstruct the epicardial activation sequence during atrial fibrillation in the time domain, studying different AF mechanisms and the effect of different strategies of AF ablation for a specific instant time or only considering visible specific organized patterns [5,6,15], like rotors, ectopic beats or macroreentrants, observable only in a few seconds time

window. However, these results not correspond with the complex propagation patterns recorded epicardially in AF patients [7], which according to our simulation results, cannot be inverse-reconstructed accurately in the voltage and phase domain due to the spatial smoothing introduced by the regularization of the system before the inverse problem resolution.

There is experimental and clinical data supporting that in many cases AF is maintained by a region with the highest activation rate [4]. Ablation of the highest DF in the atria has shown to be an effective therapy for terminating with the arrhythmia [4]. In this work we compared the noninvasive AF reconstruction error for the voltage, phase and frequency domain by solving the inverse problem of the electrocardiography, determining their percentage error and noise sensitivity.

This work proves that the inverse estimation of spectral features of atrial electrograms during AF is more accurate than the estimation of temporal-based features such as isopotential or phase maps. The smoothing effect of the body and the regularization parameter, more pronounced for a higher noise level in the ECGs, is more critical for the voltage and the phase domain.

Atrial high-frequency sources can be identified noninvasively by solving the inverse problem of the electrocardiography, with a better accuracy than with temporal-based methods. Noninvasive computation of DF maps prior to an ablation procedure may help in patient selection and procedure planning.

Acknowledgements

This work was partially supported by Spanish Ministry of Education (FPU-2012), “Universitat Politècnica de València” (PAID-2009-2012 and PAID-05-12) and the “Generalitat Valenciana” (GV/2012/039).

References

- [1] Calkins H, Brugada J, Packer DL et al. HRS/EHRA/ECAS Expert consensus statement on catheter and surgical ablation of atrial fibrillation: Recommendations for personnel, policy, procedures and follow-up. *Heart Rhythm* 2007;4:816-61.
- [2] Atienza F, Almendral J, Moreno J, Vaidyanathan R, Talkachou A, Kalifa J, Arenal A, Villacastin J.P, Torrecilla E.G, Sanchez A, Ploutz-Snyder R, Jalife J, Berenfeld O. Activation of inward rectifier potassium channels accelerates atrial fibrillation in humans-Evidence for a Reentrant mechanism. *Circulation* 2006;114:2434-42.
- [3] Haïssaguerre M, Jais P, Shah D, Takahashi A, Hocini M, Quiniou G, Garrigue S, Le Mouroux A, Le Métayer P, Clémenty J. Spontaneous initiation of atrial fibrillation by ectopic beats originating in the pulmonary veins. *N Engl J Med* 1998;339:659-66.
- [4] Atienza F, Almendral J, Jalife J, Zlochiver S, Ploutz-Snyder R, Torrecilla E, Arenal A, Kalifa J, Fernandez Aviles F, Berenfeld O. Real-time dominant frequency mapping and ablation of dominant frequency sites in atrial fibrillation with left-to-right frequency gradients predicts long-term maintenance of sinus rhythm. *Heart Rhythm* 2009;6:33-40.
- [5] Haïssaguerre M, Hocini M, Shah A. J, Derval N, Sacher F, Jais P, Dubois R. Noninvasive panoramic mapping of human atrial fibrillation mechanisms: A feasibility report. *JCE* 2013;24:711-7.
- [6] Cuculich PS, Wang Y, Lindsay BD, Faddis MN, Schuessler RB, Damiano Jr RJ, Li L, Rudy Y. Noninvasive characterization of epicardial activations in humans with diverse atrial fibrillation patterns. *Circulation* 2010;122:1364-72.
- [7] Allesie MA, de Groot NM, Houben RP, Schotten U, Boersma E, Smeets JL, Crijns HJ. Electropathological substrate of long-standing persistent atrial fibrillation in patients with structural heart disease: longitudinal dissociation. *Circ Arrhythm Electrophysiol* 2010;3:606-15.
- [8] Rodrigo M, Guillem M.S, Climent AM, Pedrón-Torrecilla J, Liberos A, Millet J, Fernández-Avilés, Atienza F, berenfeld O. Body surface localization of left and right atrial high-frequency rotors in atrial fibrillation patients: A clinical-computational study. *Heart Rhythm* 2014;11:1584-91.
- [9] Geselowitz DB. On bioelectric potentials in an inhomogeneous volume conductor. *Biophysical Journal* 1967;7:1-11.
- [10] Horáček B.M, Clements J.C. The inverse problem of electrocardiography: a solution in terms of single- and double-layer sources on the epicardial surface. *Mathematical Biosciences* 1997;144:119-54.
- [11] Hansen PC, O’Leary DP. The use of the L-curve in the regularization of discrete ill-posed problems. *SIAM J Sci Stat Comput* 1993; 14:1487-1503.
- [12] Harrild DM, Henriquez CS. A computer model of normal conduction in the human atria. *Circ Res* 2000; 87:E25-E36.
- [13] Courtemanche M, Ramirez R.J, Nattel S. Ionic mechanisms underlying human atrial action potential properties: Insights from a mathematical model. *Am J Physiol -Heart Circul Physiol* 1998;275:H301-H321.
- [14] Garcia VM, Liberos A, Climent AM, Vidal A, Millet J, González A. An adaptive step size GPU ODE solver for simulating the electric cardiac activity. *Computing in Cardiology* 2011;38:233-6.
- [15] Pedrón-Torrecilla J, Climent A, Liberos A, Pérez-David E, Millet J, Atienza F, Guillem MS. Non-invasive estimation of the activation sequence in the atria during sinus rhythm and atrial tachyarrhythmia. *Computing in Cardiology* 2012; 39:901-4.

Address for correspondence.

Jorge Pedrón Torrecilla
 Universitat Politècnica de València. Ed. 8G. Bio-ITACA
 Camino de Vera s/n. CP: 46022. Valencia, Valencia, Spain
 jorpedto@itaca.upv.com